Construction and Building Materials 225 (2019) 649–660

Contents lists available at ScienceDirect

Construction and Building Materials

journal homepage: www.elsevier.com/locate/conbuildmat

Assessment of existing micro-mechanical models for asphalt mastic considering inter-particle and physico-chemical interaction

Xiaoyan Ma [a], Huaxin Chen [a,*], Pingwen Yang [b], Mingliang Xing [a], Dongyu Niu [a], Shujuan Wu [a,c]

[a] Chang'an University, Engineering Research Center of Transportation Materials, Ministry of Education School of Materials Science and Engineering, Xi'an 710064, China
[b] Research and Development Center of Transport Industry of Technologies, Materials and Equipments of Highway Construction and Maintenance, Gansu Road & Bridge Construction Group Co., Ltd, Lanzhou 730030, China
[c] School of Civil Engineering, Lanzhou University of Technology, No. 287, Langongping Road, Qilihe District, Lanzhou, 730031 Gansu, China

HIGHLIGHTS

- Three micromechanical models was selected to predict the asphalt mastic behavior.
- GSCG gave the most accuracy modulus prediction of mastic with low filler fraction.
- J-C model cannot predict modulus of mastic with high filler fraction.
- Phy-C gave a good modulus prediction for mastic with moderate filler fraction.
- Prediction accuracy deteriorated severely with the increase of filler fraction.

ARTICLE INFO

Article history:
Received 2 April 2019
Received in revised form 16 June 2019
Accepted 19 July 2019
Available online 25 July 2019

Keywords:
Asphalt mastic
Micromechanical model
Physico-chemical interaction
Particle interaction

ABSTRACT

Micromechanical models have been used since the 1990s to predict the properties of asphalt mastic. However, most of these models are found to be unsatisfactory in predicting the mastic's properties because the models were derived from the research of particle-filled composites that did not take into account the asphalt-filler physico-chemical interactions and particle interactions. In this paper, three micro-mechanical models for predicting the complex shear modulus master curve of asphalt mastic are evaluated: the generalized self-consistent scheme model, the four-phase micro-mechanical model, and the particle interaction model. All three micro-mechanical models are based on the mechanical properties of their constituent materials as well as the filler-asphalt physiochemical interactions and the particle interactions. Two virgin asphalt binders and two polymer modified asphalt binders were selected to fabricate 16 mastics of four different filler volume fractions. The accuracy of prediction was evaluated by comparing the relative differences between the experimental complex shear modulus master curves and that predicted by the models. The results suggest that (1) the generalized self-consistent scheme model have a satisfactory prediction at a low filler volume fraction, but their accuracy is significantly affected by frequency; (2) the particle interaction model cannot calculate the complex shear modulus of mastic with a filler volume fraction of more than 0.53; (3) the four-phase model shows a precise forecast of complex shear modulus for mastic with moderate and high filler volume fractions; and (4) for all of the three models, the deviations increase severely with the increase of the filler volume fraction.

1. Introduction

Asphalt mastic is a combination of asphalt binder and mineral filler smaller than 0.075 mm. The primary use of asphalt mastic is to combine both the coarse and fine aggregates together to create asphalt concrete, which means the asphalt mastic serves as the binding agent. Traditionally, investigations into the fundamental behavior of asphalt mixtures have been based on mixture experiments or through experiments only on asphalt binders. However, the observed properties of asphalt binders are not important to the behavior of the asphalt mixture because any observations of the asphalt binders must be tempered by the physico-chemical interactions occurring between the asphalt and the mineral fillers [1]. Studies on the multiscale behaviors of asphalt materials proved that the rheological properties of asphalt mastic noticeably influenced the performance of asphalt mixtures [2–5]. Therefore, an

* Corresponding author at: Middle Section of Nan Erhuan Road, Xi'an City, Shannxi Province 720064, China.
E-mail address: chenhx_paper@163.com (H. Chen).

https://doi.org/10.1016/j.conbuildmat.2019.07.227
0950-0618/

increasing number of researchers are focused on understanding the behavior of asphalt mastic and the research involves the interaction between asphalt and filler, the factors that influence the rheological properties of mastic, and the models that can be used to predict the performance of the mastic. Among these studies, the prediction of the effective complex shear modulus of asphalt mastic is of great interest to researchers because this prediction enable many useful engineering tasks as selecting source materials (asphalt binder and mineral filler) more appropriately; improving the design of asphalt mastic and mixture within the context of multiscale approaches; promoting the development of asphalt materials to achieve desirable properties.

The viscoelastic performance of asphalt mastic depends not only on the properties of the asphalt binder and filler but also on the microstructural aspects (distribution and shape of fillers). Therefore, micromechanical models could be used as a powerful tool to predict the effective behavior of the mastic based on particular assumptions and simplifications. Buttlar and Roque were the first to recognize the potential of micromechanical models for predicting the behavior of asphalt mastics and mixtures [6]. In 1996, they divided the models into two categories: arbitrary phase geometry models and spherical inclusion models. Their study indicated that these models showed bright prospects when making a reasonable approximation of taking asphalt mastic as a system of rigid particles floating in a softer matrix.

In 1999, Buttlar applied the generalized self-consistent scheme (GSCS) model and a simple exponential model to predict the stiffening effects of various mineral fillers on an virgin asphalt binder [7]. He found that the GSCS model underestimated the stiffening effect of the mineral filler, particularly at a high filler volume fraction. Also, the calculated value of the complex shear modulus based on the GSCS model was only related to the volume fractions and not to the chemical properties and the particle sizes of the fillers. This means that different fillers with the same volume fraction had the same stiffening effect, which is obviously inconsistent with the truth. Therefore, Buttlar introduced a definition of the effective volume concentration of filler to improve the prediction and calculation of the effective volume fraction was based on the influenced asphalt layer's thickness. Since then, GSCS has become one of the most popular models for the prediction of asphalt mastic's effective modulus.

However, the GSCS model is cumbersome and inconvenient for routine use because so many computations are involved. To simplify these calculations, in 2002, Shashidhar and Shenoy proposed a simplified GSCS model based on the assuming that the modulus of the filler is far greater than that of the asphalt binder [8]. According to this simplified GSCS model, the stiffening effect of filler to asphalt was only related to the Poisson ratio of the asphalt and filler volume fractions instead of the other constituent properties such as the filler and asphalt modulus. To modify the simplified GSCS model, the effective filler volume fraction was introduced and the subsequent calculations were related to the maximum volume fraction of the filler. Now, the GSCS and simplified GSCS models are two of the most widely used models.

The existence of physical-chemical interaction between asphalt and mineral filler has been proved and a consensus was reached that filler-asphalt interaction played an important role in the performance of asphalt mastic. The interaction between asphalt and filler was defined as the rearrangement of asphalt binder's chemical components on the surface of filler [9]. Guo's investigation of the thin films of an asphalt binder interfaced with the surface of aggregates quantified the effect of the interaction [10,11]. Then, using atomic force microscope (AFM), he directly characterized the morphology and mechanical property of asphalt binder at different distances of filler surface and concluded that the effected thickness of binder–filler interaction was around 1 μm [12] and increasing the polar components ratio of asphalt binder as well as raising the specific surface area of fillers could increase the interaction degree between asphalt binder and mineral fillers [13,14]. Zhang proved that SiO_2 content and asphalt components had various levels of effects on the asphalt and filler interaction ability [15]. Therefore, based on the GSCS model, Underwood and Kim put forth the filler-asphalt physical-chemical interaction into a complex shear modulus prediction and built a new four-phase model: Phy-C model [16]. The microstructure of asphalt mastic consisted four phase as mineral filler, adsorbed asphalt binder, non-adsorbed asphalt binder and effective medium. In this model, a third phase which represent the physical-chemically influenced layer on the filler surface was taken into account. Then, the Phy-C model was applied to predict the stiffening effect of filler across a range of volumetric concentrations from 0.10 to 0.60.

In addition to the spherical inclusion model (GSCS), the arbitrary phase geometry models were applied and developed for the predictions of the performance of the asphalt mastic. According to the theory, mastic could be considered as a mineral filler/asphalt composite and mineral particle interaction can be treated as interaction problem of two elastic spherical particles embedded in matrix. Based on Ju and Chen's study of the complex modulus predictions for the random heterogeneous multiphase materials [17,18], Pei and Zhang proposed a new micromechanical model by taking into consideration the inter-particle interactions and the effective elastic modulus of asphalt mastic and mixture were predicted according to the probabilistic pairwise particle interaction mechanism and the localization relation of elastic particles [19–22]. A new parameter that represented Young' modulus of asphalt mastic was employed to reflect these inter-particle interactions. Compared with the Mori-Tanaka (M-T) [23] model and the differential scheme effective medium (DSEM) model [24] based on a single inclusion, the new model provided a better estimation of the complex shear modulus of mastics.

Besides these micromechanical models, Tehrani applied a two-dimensional/three-dimensional biphasic models and a numerical model to predict the dynamic modulus of mastic based on the finite element method. However, the results showed that both of the predicted results were placed below the experimental results [25–27].

Hajikarimi employed the finite-element method to predict the modulus of polymer-modified asphalt mastics with two very low filling ratios of 18% and 35%, and the results showed that a higher difference existed between the numerical results and the experimental observation with a filling ratio of 35% [28]. Al-Khateeb derived a simplified exponential model to predict the modulus of mastic from that of asphalt, quality, and density of filler [8]. Reliability analysis of the model was based on mastics with filler volume fractions less than 0.3. Yan also derived a simple exponential model to predict the modulus of mastic at fixed frequency and temperature [29].

As there existed many models for elastic composite materials' modulus prediction, some researchers are devoted to finding an appropriate model to estimate the viscoelastic composite (asphalt mastic) modulus within these existing models. For example, Kim demonstrated the applicability of the rheology-based model (Nielsen model), linear viscoelastic conversion of the analytical elastic model (Hashin model), and Christensen and Lo model to the modulus prediction of asphalt mastic with filler volume fractions less than 25% [30]. Yin assessed the accuracy of the dilute model (DM), self-consistent model (SCM), Mori-Tanaka model (MT), and generalized self-consistent model (GSCM) on the predictions of mastic modulus [31]. The results showed that the DM and CSM models overestimated the modulus and the MT and GSCM underestimated it. Brinson and Lin also examined the MT and the finite element method for determination of the effective properties of mastic [32].

As discussed above, the remaining problems are as follows. (1) Most of these micromechanical models, simplified exponential models, and finite element-based models have been evaluated at fixed temperatures and frequencies or for a relatively narrow range of frequencies. In practice, asphalt mastic is subjected to a wide range of frequencies and temperatures on pavements, so a deep insight into the modulus prediction model is necessary. (2) Almost all of the existing models are focused on modulus prediction of mastics fabricated by virgin asphalt binders. Little was know about these models' application on polymer-modified asphalt mastics, such as the SBS modified asphalt and high-viscosity asphalt mastic. (3) Except for a few studies, most of the investigations on modulus prediction models has involved mastics with filler volume fractions of not more than 0.4. However, the appropriate filler volume fraction of mastic ranges from about 0.23 to 0.60 for most of asphalt mixtures. So, the primary purpose of this study is to evaluate the application of the existed prediction models for both the virgin asphalt and modified asphalt mastics of various filler volume fractions for a wide range of frequencies.

2. Materials and methods

2.1. Materials

Two virgin asphalt binders (SK90 and KL70) and two polymer modified asphalt binders (SBS modified asphalt and HV asphalt) were selected in this study, as they are the most commonly used asphalt binders in pavement construction in China. SK90 an 80/100 penetration grade asphalt binder produced by SK Company of Korea and KL70 is a 60/80 penetration grade asphalt binder produced by Petrochina Company. SBS modified asphalt is fabricated in laboratory and HV asphalt is a high viscosity asphalt binder produced by Shell Oil Company. The performances of these four asphalt binders are presented in Table 1. The four asphalt binders and one limestone filler (<0.075 mm in diameter) were used to fabricate mastic of different filler volume fractions. The filler's density was 2.685 g/cm^3, and its specific surface area was 482 m^2/kg, testing of which followed the specification of ASTM C2040.2011.

According to the "Technical Specification for Construction of Highway Asphalt Pavement (JTG F40-2004)" of China, the recommended range of filler/asphalt (by weight) is from 0.6 to 1.6 for hot asphalt mixture and from 1.0 to 1.8 for Slurry seal (SE-1). Therefore, four filler/asphalt ratio (by weight) of 0.6, 1.0, 1.4 and 1.8 were employed. And then the filler/asphalt ratios were converted to filler volume fractions (filler/mastic by volume) as 0.23, 0.38, 0.53, and 0.68.

The fabrication of the asphalt mastic was done in the laboratory using a small electric mixer. Before mixing, the virgin asphalt binders and modified asphalt binders were melted in ovens at temperatures of 110 °C and 165 °C, respectively. To prevent a temperature decrease of the mixture caused by the addition of the mineral filler, which would make it difficult to mix asphalt binder and filler well, the filler was heated at the same temperature as the corresponding asphalt binder. Then the filler was added gradually to the melting asphalt by stirring and heating. The whisking was kept up for 15 min until the mixture was homogeneous and texture of the loose mastic was carefully observed during the pour to avoid any inhomogeneities in the sample. A minimum of three replicates were prepared for each test.

2.2. Experiment

Amplitude sweep and temperature-frequency sweep tests were conducted using the AR2000 dynamic shear rheology (DSR) from TA Co. Ltd. The tests were carried out with 25 mm diameter, 1 mm gap geometry between 30 °C and 70 °C, and with 25 mm diameter, 2 mm gap geometry less than 30 °C. The amplitude sweep tests were performed at a temperature of 15 °C and a frequency of 0.1–100 rad/s. Then, based on the linear viscoelastic strain limit determined by amplitude sweep tests, the temperature-frequency sweep tests (temperatures: 15 °C–70 °C; frequency: 0.1–100 rad/s) were applied to the asphalt binders and mastics to obtain complex shear modulus and phase angle. A minimum of three replications were tested for each condition. The rheological properties of the asphalt binders and mastics were determined following the test protocol based on the EN 14770.

3. Theoretical background

3.1. GSCS model

The GSCS model consists of the single composite sphere embedded in the infinite medium of unknown effective properties (Fig. 1) [33]. Derivation of the formula is based on the hypothesis that a particle is coated with a material that has the same effective modulus with the particle itself. The ratio of radii for the particle and coating is presented as $a^3/b^3 = c$, and c is the volume fraction of particles. The GSCS model can be expressed as follows:

$$A\left(\frac{G_c}{G_m}\right)^2 + 2B\left(\frac{G_c}{G_m}\right) + C = 0 \tag{1}$$

$$\begin{aligned} A = {} & 8\left(\tfrac{G_p}{G_m}-1\right)(4-5v_m)\eta_1\varphi^{10/3} - 2\left[63\left(\tfrac{G_p}{G_m}-1\right)\eta_2 + 2\eta_1\eta_2\right]\varphi^{7/3} \\ & + 252\left(\tfrac{G_p}{G_m}-1\right)\eta_2\varphi^{5/3} - 50\left(\tfrac{G_p}{G_m}-1\right)(7-12v_m+8v_m^2)\eta_2\varphi \\ & + 4(7-10v_m)\eta_1\eta_2 \end{aligned} \tag{2}$$

$$\begin{aligned} B = {} & -4\left(\tfrac{G_p}{G_m}-1\right)(1-5v_m)\eta_1\varphi^{10/3} + 4\left[63\left(\tfrac{G_p}{G_m}-1\right)\eta_2 + 2\eta_1\eta_2\right]\varphi^{7/3} \\ & -504\left(\tfrac{G_p}{G_m}-1\right)\eta_2\varphi^{5/3} + 150\left(\tfrac{G_p}{G_m}-1\right)(3-v_m)v_m\eta_2\varphi \\ & +3(15v_m-7)\eta_2\eta_3 \end{aligned} \tag{3}$$

$$\begin{aligned} C = {} & 4\left(\tfrac{G_p}{G_m}-1\right)(5v_m-7)\eta_1\varphi^{10/3} - 2\left[63\left(\tfrac{G_p}{G_m}-1\right)\eta_2 + 2\eta_1\eta_2\right]\varphi^{7/3} \\ & +252\left(\tfrac{G_p}{G_m}-1\right)\eta_2\varphi^{5/3} + 25\left(\tfrac{G_p}{G_m}-1\right)(v_m^2-7)\eta_2\varphi - (7+5v_m)\eta_2\eta_3 \end{aligned} \tag{4}$$

$$\begin{aligned} \eta_1 = {} & \left(\frac{G_p}{G_m}-1\right)(49-50v_p v_m) + 35\left(\frac{G_p}{G_m}\right)(v_p-2v_m) \\ & + 35(2v_p-v_m) \end{aligned} \tag{5}$$

Table 1
Properties of Asphalt Binders.

Type	Penetration 25 °C/0.1 mm	Soften Point °C	Ductility cm	PG performance grade °C
SK90 asphalt	83.0	45.5	>100 (15 °C)	52–28
KL70 asphalt	65.5	48.0	>100 (15 °C)	58–22
SBS modified asphalt	62.0	84.5	42 (5 °C)	76–28
HV asphalt	64.5	82.0	36 (5 °C)	76–22

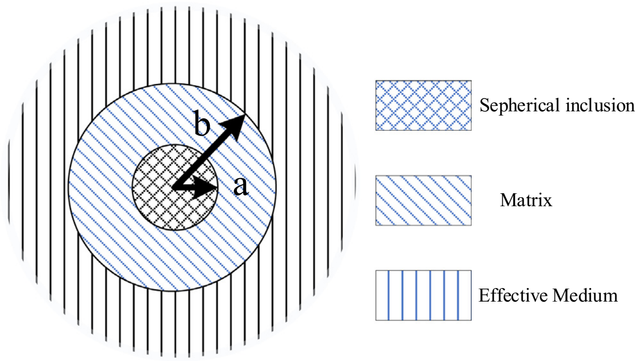

Fig. 1. Generalized self-consistent scheme model for particular composite [7,23].

$$\eta_2 = 5v_p\left(\frac{G_p}{G_m} - 8\right) + 7\left(\frac{G_p}{G_m} + 4\right) \tag{6}$$

$$\eta_3 = \left(\frac{G_p}{G_m}\right)(8 - 10v_m) + (7 - 5v_m) \tag{7}$$

$$G_c = \frac{\sqrt{B^2 - AC} - B}{A} G_m \tag{8}$$

where G_c and G_m is the complex shear modulus of asphalt mastic and asphalt matrix; v_p and v_m are the Poisson ratios of filler particles and asphalt matrix; φ is filler volume fraction.

When GSCS was applied to predict the modulus of asphalt mastic, it was found that the predicted results were far below the experimental results, so Buttlar replaced the particle volume fraction in the original GSCS with "effective filler volume fraction", which was related to the physical-chemical interaction between asphalt binder and filler. The difference between the original filler volume fraction and the effective filler volume fraction can be likened to "apparent immobilized asphalt, V_{imm}" [7]. The effective filler volume fraction can be calculated as follows:

$$V_{imm} = \varphi_e - \varphi \tag{9}$$

The ratio of immobilized asphalt relative to volume concentration of filler can be calculated as follows:

$$R_{imm} = \frac{V_{imm}}{\varphi} \tag{10}$$

When the thickness of the rigid layer of asphalt binder on the filler was determined, the calibrated effective volume concentration can be calculated as follows:

$$\varphi_e = \varphi(1 + R_{imm}) \tag{11}$$

If the surface area of the filler is known, the apparent rigid layer thickness can be computed as follows:

$$t_{ra} = \frac{\text{Volume of apparent immobilized asphat per cm}^{\text{cm}}}{\text{surface area of filler per cm}^{\text{cm}}} \tag{12}$$

$$t_{ra}\,(\text{microns}) = \frac{(\varphi_e - \varphi)}{\varphi \times g_s \times \text{surface area}\,(\text{m}^2/\text{g}) \times (100\,\text{cm/m})^3} \times 10^6\,\mu\text{m/m} = \frac{\varphi_e - \varphi}{\varphi \times g_s \times \text{surface area}\,(\text{m}^2/\text{g})} \tag{13}$$

where g_s is the filler specific gravity.

Calculation of the apparent rigid layer thickness is based on the specific gravity, surface area and the effective filler volume fraction. And the effective filler volume faction was determined by the dispersed state of filler in asphalt.

3.2. Inter-particle interaction model

According to Ju and Chen's micromechanical framework of two particles' interactions that are embedded into an elastic matrix (Fig. 2), the ensemble-average solution can be obtained by integrating all possible positions of particle x_2 when the location of particle x_1 is fixed. The conditional probability function is determined by the shape and volume fraction of the particles.

Based on the mechanism of the probabilistic pairwise particle interactions, the constitutive model is determined and thus the modulus prediction model is presented, which involves two-phase composites containing randomly located spherical particles. Asphalt mastic is a typical composite material in which the mineral filler is the elastic spherical particles and the viscoelastic asphalt binder can be regarded as the matrix [14]. Based on Ju and Chen's micromechanical model the effective shear modulus of asphalt mastic could be expressed as follows:

$$G_c = G_m\left[1 + \frac{30(1 - v_0)\varphi\gamma_2}{\beta - 4(4 - 5v_0)\varphi\gamma_2}\right] \tag{14}$$

$$\gamma_2 = \frac{1}{2} + \frac{5\varphi}{4\beta^2} Y(g)\xi_2 \tag{15}$$

$$\xi_2 = 6(25 - 34v_0 + 22v_0^2) - \frac{36\alpha}{2\alpha + 2\beta}(1 - 2v_0)(1 + v_0) \tag{16}$$

$$\alpha = 2(5v_0 - 1) + 10(1 - v_0) \cdot \left(\frac{k_m}{k_p - k_m} - \frac{G_m}{G_p - G_m}\right) \tag{17}$$

$$\beta = 2(4 - 5v_0) + 15(1 - v_0) \cdot \frac{G_m}{G_p - G_m} \tag{18}$$

where k_m and k_p is the bulk modulus of asphalt and filler; The unknown parameter Y(g) is the Young modulus.

Y(g) is related to the overall interactions of the particles and depends on the filler volume fraction and particle shape. In asphalt mastic, the mineral filler's particles are assumed to be spherical. According to Chen, Y(g) increases with the filler volume fraction and has a minimum value of 1/24 [18]. To simplify the calculation, Pei defined a new parameter ς to represent value of Y(g) as 1/24, 1/20, 1/16, 1/12 as the filler volume fraction increased from 0.23 to 0.68[19].

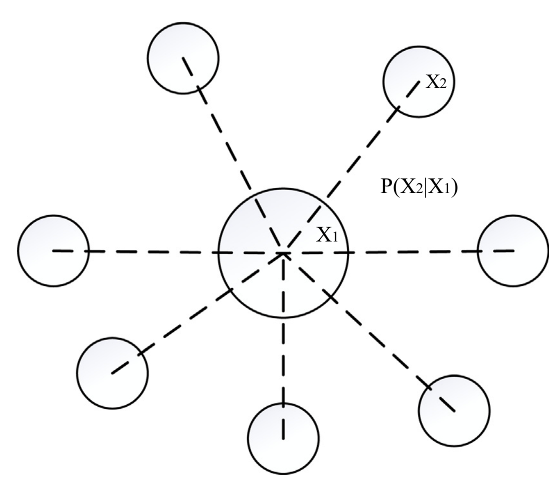

Fig. 2. Schematic diagram for the probabilistic two-particle interaction [14].

3.3. Phy-C model

Existed evidence suggests that the interactions between the asphalt and the filler significantly affected the properties of the final mastic [13,34,35]. The three-phase GSCS model applied by Buttlar involved this physico-chemical interaction and took the adsorbed rigid layer into account. However, the three-phase GSCG model did not take the property and amount of non-adsorbed asphalt influenced into consideration as well as the mechanics of the adsorbed and non-adsorbed asphalt within mastic. Based on the equivalent medium micro-mechanicals, the four-phase model microstructure consists of a mineral filler, an adsorbed rigid asphalt layer, a non-adsorbed asphalt layer, and an effective medium. As the four-phase model took the physical-chemical interaction of asphalt binder and filler into account, it was also named the Phy-C model. The schematic diagram of filler asphalt interactions and the Phy-C model are shown as Figs. 3 and 4.

The formulation of micro-mechanical model employed for the calculation of the effective property of the four-phase microstructural composite is similar to GSCS model. Derivation of the model involved the amount and properties of adsorbed and non-adsorbed asphalt. The four-phase micro-mechanical model could expressed as follows:

$$Q\left(\frac{G_c^*}{G_m^*}\right)^2 + R\left(\frac{G_c^*}{G_m^*}\right) + S = 0 \quad (19)$$

$$\begin{aligned} Q = {} & 4(1-2v_{b-na}^*)(7-10v_{b-na}^*)Z_{12} + 20\left(7-12v_{b-na}^* + 8(v_{b-na}^*)^2\right)Z_{42} \\ & + 12(1-2v_{b-na}^*)(Z_{14}-7Z_{23}) + 20(1-2v_{b-na}^*)Z_{13} \\ & + 16(4-5v_{b-na}^*)(1-2v_{b-na}^*)Z_{43} \end{aligned} \quad (20)$$

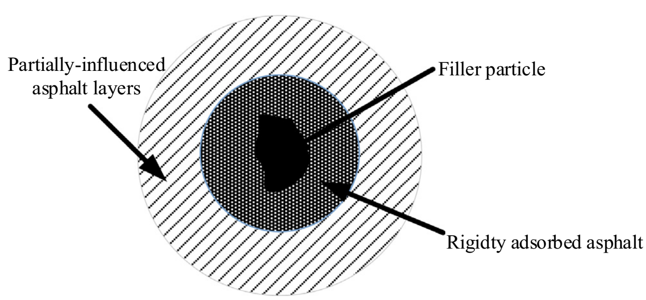

Fig. 3. Schematic diagram for filler-asphalt interaction.

$$\begin{aligned} R = {} & 3(1-2v_{b-na}^*)(15v_{b-na}^*-7)Z_{12} + 60(v_{b-na}^*-3)v_{b-na}^*Z_{42} \\ & - 24(1-2v_{b-na}^*)(Z_{14}-7Z_{23}) - 40(1-2v_{b-na}^*)^2 Z_{13} - 8(1 \\ & - 5v_{b-na}^*)(1-2v_{b-na}^*)Z_{43} \end{aligned} \quad (21)$$

$$\begin{aligned} S = {} & -(1-2v_{b-na}^*)(7+5v_{b-na}^*)Z_{12} + 10(7-(v_{b-na}^*)^2)Z_{42} \\ & + 12(1-2v_{b-na}^*)(Z_{14}-7Z_{23}) + 20(1-2v_{b-na}^*)^2 Z_{13} \\ & - 8(7-5v_{b-na}^*)(1-2v_{b-na}^*)Z_{43} \end{aligned} \quad (22)$$

$$Z_{\alpha\beta} = P_{\alpha1}^{(2)}P_{\beta2}^{(2)} - P_{\beta1}^{(2)}P_{\alpha2}^{(2)} \quad (23)$$

$$P^{(2)} = \prod_{j=1}^{2} M^{(1)}M^{(2)} = L_2^{-1}(R_1)L_1(R_1)L_3^{-1}(R_2)L_2(R_2) \quad (24)$$

where, $L_2(R_1), L_1(R_1), L_3(R_2)$ and $L_2(R_2)$could be expressed as follows.

$$L_2(R_1) = \begin{bmatrix} R_1 & -\frac{6v_2}{1-2v_2}R_1^3 & \frac{3}{R_1^4} & \frac{5-4v_2}{1-2v_2}\frac{1}{R_1} \\ R_1 & -\frac{7-4v_2}{1-2v_2}R_1^3 & -\frac{2}{R_1^4} & \frac{2}{R_1^2} \\ G_2 & \frac{3G_2v_2}{1-2v_2}R_1^2 & -\frac{12G_2}{R_1^5} & \frac{2G_2(v_2-5)}{1-2v_2}\frac{1}{R_1^3} \\ G_2 & -\frac{G_2(7+2v_2)}{1-2v_2}R_1^2 & \frac{8G_2}{R_1^5} & \frac{2G_2(v_2+1)}{1-2v_2}\frac{1}{R_1^3} \end{bmatrix} \quad (25)$$

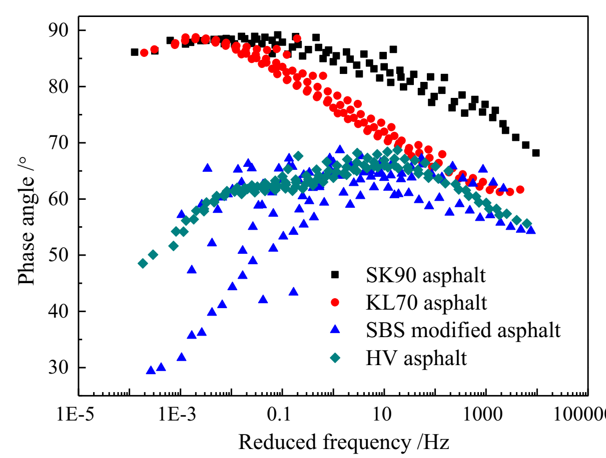

Fig. 5. Phase angle master curves of the four asphalt binders.

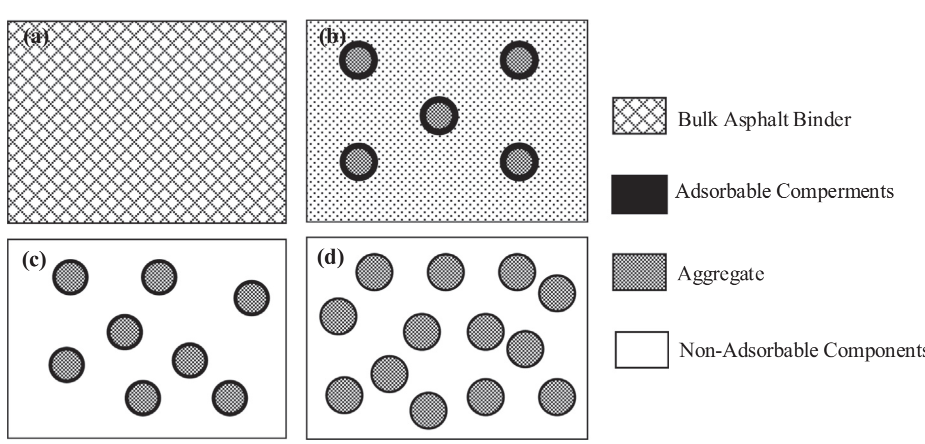

Fig. 4. Schematic representation of four-phase model of different filler volume fractions. (a) Asphalt binder. (b) Mastic with low filler volume fraction at which condition full adsorption of can be achieved with extra adsorbable components in distributed asphalt phase. (c) Mastic with moderate filler volume fraction at which condition all adsorbable components of asphalt are adsorbed. (d) Mastic with high filler volume fraction at which condition all adsorbable components are adsorbed, but the adsorbed film thickness is less than that of condition (a) and (b) [11].

$$L_1(R_1) = \begin{bmatrix} R_1 & -\frac{6v_1}{1-2v_1}R_1^3 & \frac{3}{R_1^4} & \frac{5-4v_1}{1-2v_1}\frac{1}{R_1} \\ R_1 & -\frac{7-4v_1}{1-2v_1}R_1^3 & -\frac{2}{R_1^4} & \frac{2}{R_1^2} \\ G_1 & \frac{3G_1v_1}{1-2v_1}R_1^2 & -\frac{12G_1}{R_1^5} & \frac{2G_1(v_1-5)}{1-2v_1}\frac{1}{R_1^3} \\ G_1 & -\frac{G_1(7+2v_1)}{1-2v_1}R_1^2 & \frac{8G_1}{R_1^5} & \frac{2G_1(v_1+1)}{1-2v_1}\frac{1}{R_1^3} \end{bmatrix} \quad (26)$$

$$L_3(R_2) = \begin{bmatrix} R_2 & -\frac{6v_3}{1-2v_3}R_2^3 & \frac{3}{R_2^4} & \frac{5-4v_3}{1-2v_3}\frac{1}{R_2} \\ R_2 & -\frac{7-4v_3}{1-2v_3}R_2^3 & -\frac{2}{R_2^4} & \frac{2}{R_2^2} \\ G_3 & \frac{3G_3v_3}{1-2v_3}R_2^2 & -\frac{12G_3}{R_2^5} & \frac{2G_3(v_3-5)}{1-2v_3}\frac{1}{R_2^3} \\ G_3 & -\frac{G_3(7+2v_3)}{1-2v_3}R_2^2 & \frac{8G_3}{R_2^5} & \frac{2G_3(v_3+1)}{1-2v_3}\frac{1}{R_2^3} \end{bmatrix} \quad (27)$$

$$L_2(R_2) = \begin{bmatrix} R_2 & -\frac{6v_2}{1-2v_2}R_2^3 & \frac{3}{R_2^4} & \frac{5-4v_2}{1-2v_2}\frac{1}{R_2} \\ R_2 & -\frac{7-4v_2}{1-2v_2}R_2^3 & -\frac{2}{R_2^4} & \frac{2}{R_2^2} \\ G_2 & \frac{3G_2v_2}{1-2v_2}R_2^2 & -\frac{12G_2}{R_2^5} & \frac{2G_2(v_2-5)}{1-2v_2}\frac{1}{R_2^3} \\ G_2 & -\frac{G_2(7+2v_2)}{1-2v_2}R_2^2 & \frac{8G_2}{R_2^5} & \frac{2G_2(v_2+1)}{1-2v_2}\frac{1}{R_2^3} \end{bmatrix} \quad (28)$$

In this matrix, the subscript1, 2, and 3 represent the mineral filler, adsorbed asphalt, and non-adsorbed asphalt, respectively. R_k is related to the volume fraction of a different phase and can be calculated by Eqs. (29) and (30). Values of $G_2$and G_3could be calculated by Eqs. (31) and (32).

$$R_1 = (C_v)^{1/3} \quad (29)$$

$$R_k = \left(\frac{V_k}{100} - R_{k-1}^3\right)^{1/3} \quad (30)$$

$$G_{b-a}^* = Z \times G_b^* \quad (31)$$

$$G_{b-na}^* = \frac{G_b^* \times G_{b-a}^* \times V_{b-na}}{G_{b-a}^* - G_b^* \times V_{b-a}} \quad (32)$$

where $G_{b-na}^*$is the shear complex modulus of non-adsorbed asphalt binder; G_{b-a}^* is the shear complex modulus of adsorbed asphalt binder; V_{b-a} and V_{b-na} are the volume fraction of adsorbed asphalt and non-adsorbed asphalt. Z is a coefficient, and the determination of Z at different filler volume fraction is based on following.

$$Err = \frac{2V_{b-a} \times Z(1 - \cos(\delta_b - \delta_{b-a}))}{(Z - V_{b-a})^2} \quad (33)$$

This error function was defined based on experiences, with an acceptable level of error set at 5%. In the equation, the phase angle of the adsorbed asphalt is assumed to be equal to zero degrees. Then, the phase angle of the asphalt binder and adsorbed asphalt volume fraction were substituted into Eq. (33) to calculate the value of Z. The phase angle master curve of the four asphalt binders are shown as Fig. 5. In this study, 20 phase angles for each asphalt binder were selected to calculate Z of different filler volume fractions and the Z values of different asphalt mastics are shown in Fig. 6.

The volume fraction of the adsorbed and non-adsorbed asphalt binder at different filler volume fractions were determined according to Underwood and Branthaver's studies [14]. Their research showed that the adsorbed film thickness was a constant of about 0.60μm as the filler volume fraction was less than 0.40, and then

Table 2
Volumetric content of different phases.

Filler volume fraction/%	Adsorbed asphalt/%	Non-adsorbed asphalt/%
23.0	23.5	53.5
38.0	21.0	41.0
53.0	16.0	31.0
68.0	11.0	21.0

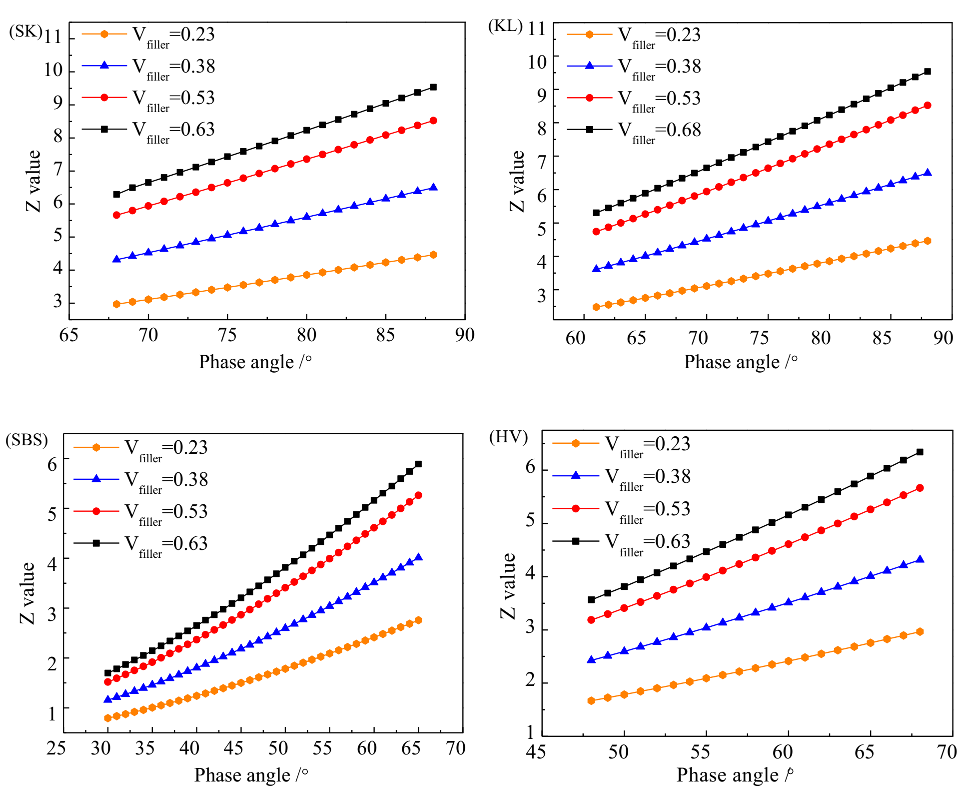

Fig. 6. Z value of the four asphalt with different filler volume fraction.

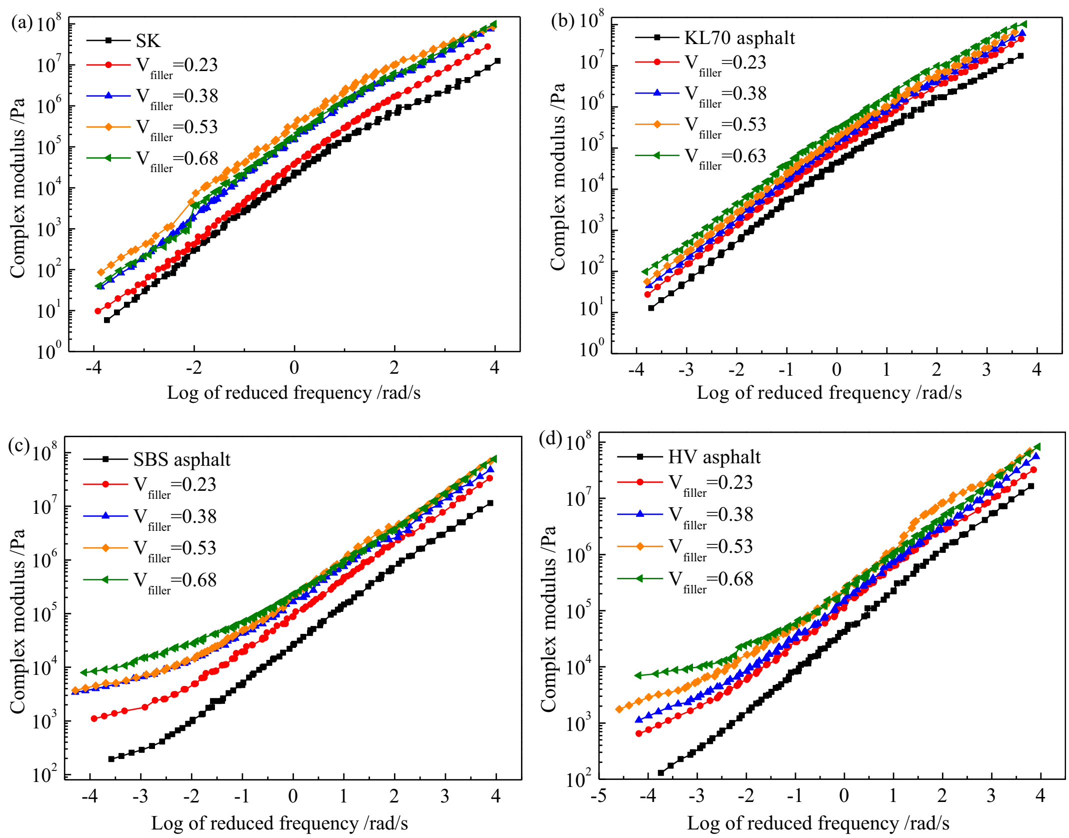

Fig. 7. Complex shear modulus master curves of (a) SK90, (b) KL70, (c) SBS modified and (d) HV asphalt and their corresponding mastics of different filler volume fraction.

the film thickness was reduced with the increase of filler volume fraction. Simultaneously, for a convenient application, the adsorbed film thickness was converted into a volume fraction. When the filler volume fraction was less than 0.30, the volume fraction of the adsorbed asphalt was almost the same as that of the filler, and therefore, in this study, the determination of the adsorbed asphalt was simplified. The volume fractions of filler, adsorbed asphalt, and non-adsorbed asphalt are listed in Table 2.

4. Results and discussion

4.1. Experimental results

The measured complex shear modulus master curves of the four asphalt binders and 16 mastics are summarized in Fig. 7. Construction of the master curve is based on the time-temperature equivalence principle to replace the effect of both frequency and temperature with a single frequency (reduced frequency). In this study, a middle-point temperature of 40 °C was selected as the reference temperature. Evaluation of the commonly used modulus master curve description models as Sigmoidal Model, the Generalized Logistic Sigmoidal Model, the Christensen-Anderson (CA) Model, and the Christensen-Anderson-Marasteanu (CAM) confirmed that the CAM model showed an outstanding correlation between measured and descriptive complex modulus [36,37]. The Christensen-Anderson-Marasteanu (CAM) model was developed by Marasteanu and Anderson to modify the previous Christensen Anderson (CA) model and Anderson study indicated that the CAM improved the description of polymer-modified asphalt as well as virgin asphalt at both low and high frequencies [36]. Therefore, in this study, CAM model was selected to describe the complex shear modulus master curve of asphalt binders and mastics. The CAM model was defined as follows.

$$G^{*} = G_{g}\left[1 + \left(\frac{f_{c}}{f}\right)^{v}\right]^{-\frac{w}{v}} \quad (34)$$

$$R = \frac{\log 2}{v} \quad (35)$$

where, $G^{*}$is the complex shear modulus; $G_{g}$is the glassy modulus as$f \to \infty$; f_{c} is the location parameter with dimensions of frequency; $f$is reduced frequency; w, v is the experimental curve fitting parameters.

4.2. Evaluation and comparison with experiments

The GSCS model, physical-chemical model, and particle interaction model were applied to predict the complex modulus of the 16 asphalt mastics. The complex shear modulus of asphalt binder, filler volume fractions, Poisson ratios of asphalt binder and filler, and the volume fraction of the adsorbed asphalt were used as inputs. Assuming the modulus of the filler was 1.90GPa, the Poisson ratios of the filler and asphalt binder are 0.35 and 0.45, respectively. Figs. 8–11 present the complex shear modulus master curves of asphalt mastics predicted by the three different models and the predicted results were compared with the experimental results.

To evaluate effective of the models, the predicted complex shear modulus was compared with that of the tested at the same frequency and temperature. The relative difference (RD) between the results obtained from experimental tests and prediction models was applied to indicate the accuracy of the prediction and RD can be calculated by Eq. (36). Smaller the absolute value of RD, more accurate the prediction. Figs. 8–11 presents the RD value of

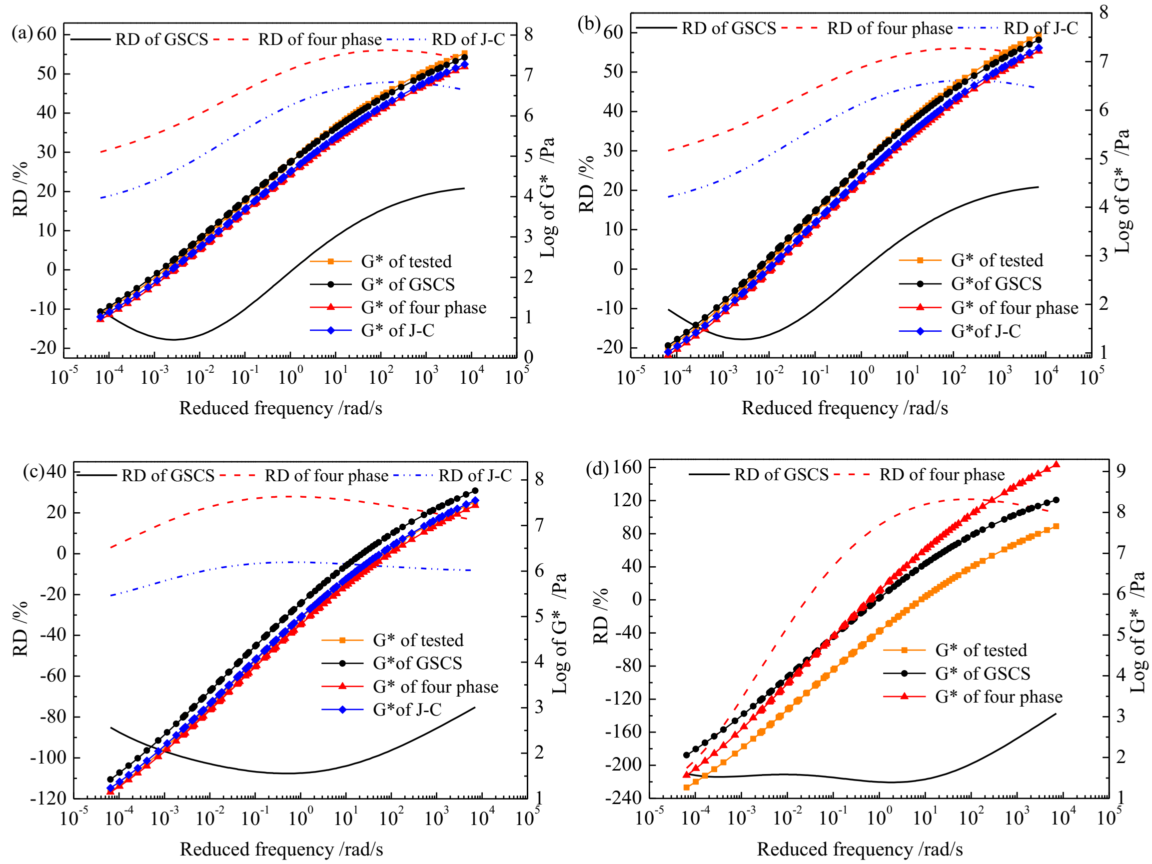

Fig. 8. Comparison of complex modulus master curves and relative difference of the tested and predicted results of SK90 asphalt mastics with filler volume fraction of (a) 0.23; (b) 0.38; (c) 0.53; (d) 0.68.

the three models as well as complex shear modulus of asphalt mastics.

$$\mathrm{RD}\ (\%) = \frac{G^*(\omega)_{(\mathrm{Tested})} - G^*(\omega)_{(\mathrm{Predicted})}}{G^*(\omega)_{(\mathrm{Tested})}} \times 100 \tag{36}$$

where, $G^*(\omega)_{(\mathrm{Tested})}$ is the complex shear modulus obtained by experiment, $G^*(\omega)_{(\mathrm{Predicted})}$ is the complex shear modulus calculated by the prediction model.

As illustrated in Figs. 8–11, comparisons of the complex shear modulus predicted by GSCS, four-phase, and J-C model with that of experimental tests showed that the predictions are all in good agreement with the experiments on a whole and the predicted dynamic modulus follows the general trend of the mastic. Even more telling was the significant differences of the RD value of the three models.

For SK90 and KL70 asphalt mastics with low filler volume fractions (less than 0.53), the value of the relative difference shows that the GSCS model overestimated the complex modulus of mastics, while the four-phase model and J-C model underestimated it. As the values of relative differences ranged from −15% to 15%, 10% to 55%, and 5% to 35% for the GSCS model, four-phase model, and J-C model, respectively, it was obvious that the GSCS model agreed better with the experimental results than the four-phase model and J-C model. For the two virgin asphalt with moderate filler volume fraction (equal to 0.53), the values of relative differences, which ranged from 200% to 50% and −90% to 70% of the GSCS model and the J-C model, showed a remarkable increase as the prediction accuracy of these two models decreased significantly. This value ranged from 5% to 30% of the four-phase model, indicated the four-phase model still exhibited a good agreement with the experimental results. For the asphalt mastics with a filler volume fraction of 0.68, the changes of the relative difference of GSCS and four-phase models showed that the prediction further deteriorated. The GSCS model highly overestimated the complex modulus for about 220%–140%. The four-phase model underestimated the complex modulus at a low frequency for 220% and then underestimated it at about 120% at high frequency. Furthermore, the predicted modulus of the J-C model was negative and that was obviously not being in accordance with the facts.

For SBS and HV asphalt mastics with four different filler volume fractions, all of the three models underestimated the complex modulus at low frequencies. Each of the three models had greater values of relative differences for the polymer modified asphalt than that of virgin asphalt mastics with the same filler volume fraction. For the SBS and HV asphalt mastics with a filler volume fraction of 0.23, the GSCS model could still make precise prediction that was the same as virgin asphalt mastics. However, with the increasing of the filler volume fraction, the four-phase model showed more obvious advantages.

Above analysis showed that there were common features and tendencies across the three approaches. Several influences of filler volume fraction and frequency on the prediction accuracy of the three model had been observed:

(1) Value of RD increased with the increase of filler volume fraction. The complex modulus predicted by GSCS, four-phase, and J-C models agreed well with the experimental results for mastics with low and moderate filler volume fractions; the value of RD significantly increased as the filler volume fraction is greater than or equal to 0.53.

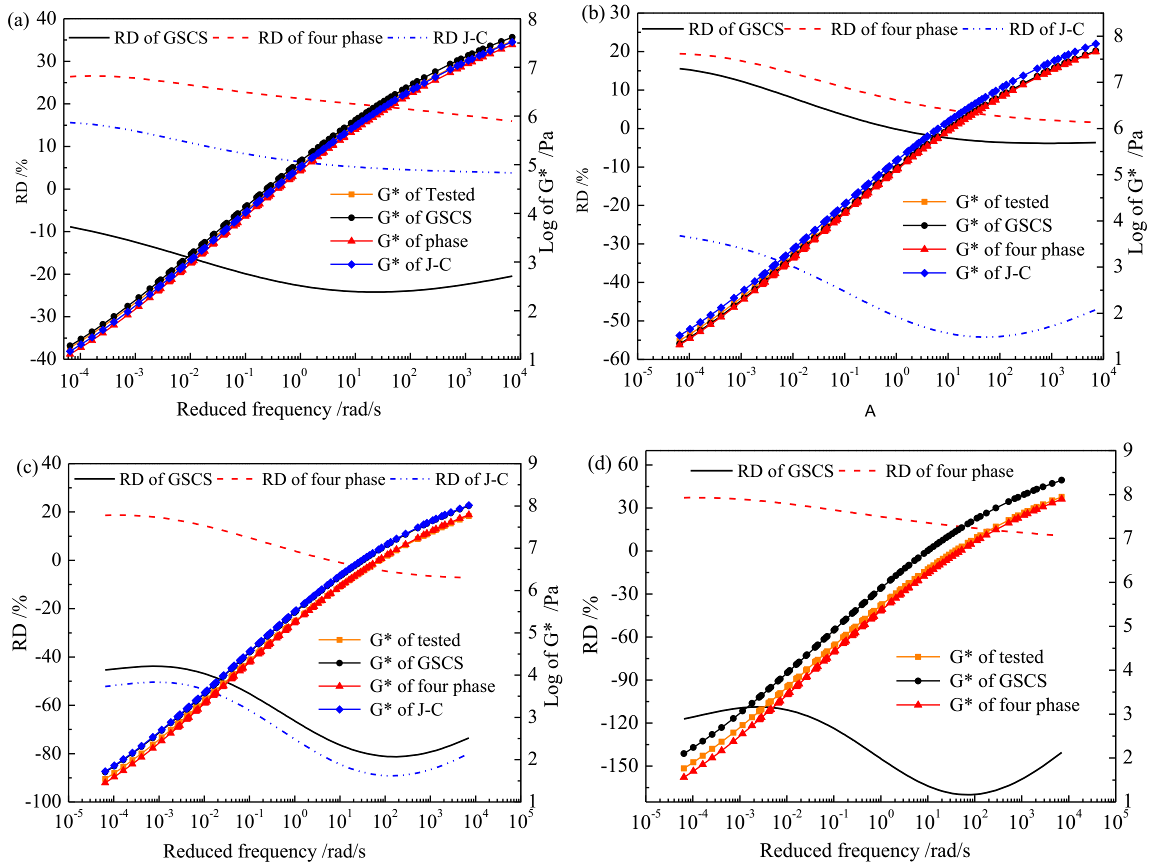

Fig. 9. Comparison of complex modulus master curves and relative difference of the tested and predicted results of KL70 asphalt mastics with filler volume fraction of (a) 0.23; (b) 0.38; (c) 0.53; (d) 0.68.

(2) For the mastics with the same filler volume fraction, as observed from the form of relative difference curves, frequency had a significant and complicated effect on the evaluation of the predicted models.
(3) All of the three models underestimated the complex modulus of polymer modified asphalt mastic at a frequency of less than 1 rad/s and a lower prediction accuracy for modified asphalt mastics than virgin asphalt mastics with the same filler volume fraction.

Micro-mechanical modeling is a powerful tool for predicting the complex modulus of asphalt mastics, and the GSCS, four-phase, and J-C models are considered as effective and reasonable methods for the mastic stiffening effect related to filler volume fractions, as well as asphalt-filler physico-chemical interactions and mineral particle interactions. The models were derived based on the some assumptions, one of the most important assumption was that the shape of filler particle was spherical. However, the mineral fillers of asphalt mastic have a very irregular shape. Therefore, one possibility is that the influence of particle shape leaded to the decreased accuracy of the prediction models. Also, with the increase of the filler volume fraction, the potential for some of the filler particles aggregating to form a large cluster could intensify and it caused the increase in the prediction error. As the mineral filler is much stiffer than asphalt binder, all of the above models assumed that the mineral filler was rigid to simplify the calculations. However, with the decreasing of temperature and the increasing of frequency, the stiffness of the asphalt binder grows rapidly. Therefore, at a low temperature (a high frequency), the rigid mineral filler assumption might not be suitable. This may be one of the explanations for the larger value of the relative differences at a higher frequency. Additionally, according to Di Benedetto's study on the complex modulus and Poisson's ratio of 50/70 penetration grade asphalt and mastics with a 32% limestone filler, the absolute value of Poisson's ratio ranges from 0.34 to 0.50, and this was a value highly dependent on frequency and temperature. At a high frequency and a low temperature, the value of Poisson's ratio tended toward 0.34, which means it was reasonable to consider the asphalt as compressible. This might be another explanation for the variations of relative differences with frequencies for all of the three models.

In addition to the three common characteristics in the three models, there are significant differences exist across the different approaches:

(1) For the three models, the maximum of the absolute value of RD for GSCS model is the smallest for either virgin asphalt and modified asphalt mastics with filler volume fraction of 0.23. It indicated that the GSCS model had the highest prediction accuracy among these models for mastics with small filler volume fraction. Meanwhile, the GSCS model also shows the smallest difference between maximum and minimum value of RD.
(2) Figs. 8–11 show the relative difference significantly increased with the growth of filler volume fraction for all the three models. However, the sensitivity of different models to filler volume fraction was significantly different. RD value of the GSCS model was more sensitive to filler volume fraction than other two models and the four phase model was insensitive to filler volume fraction compared to other two models.

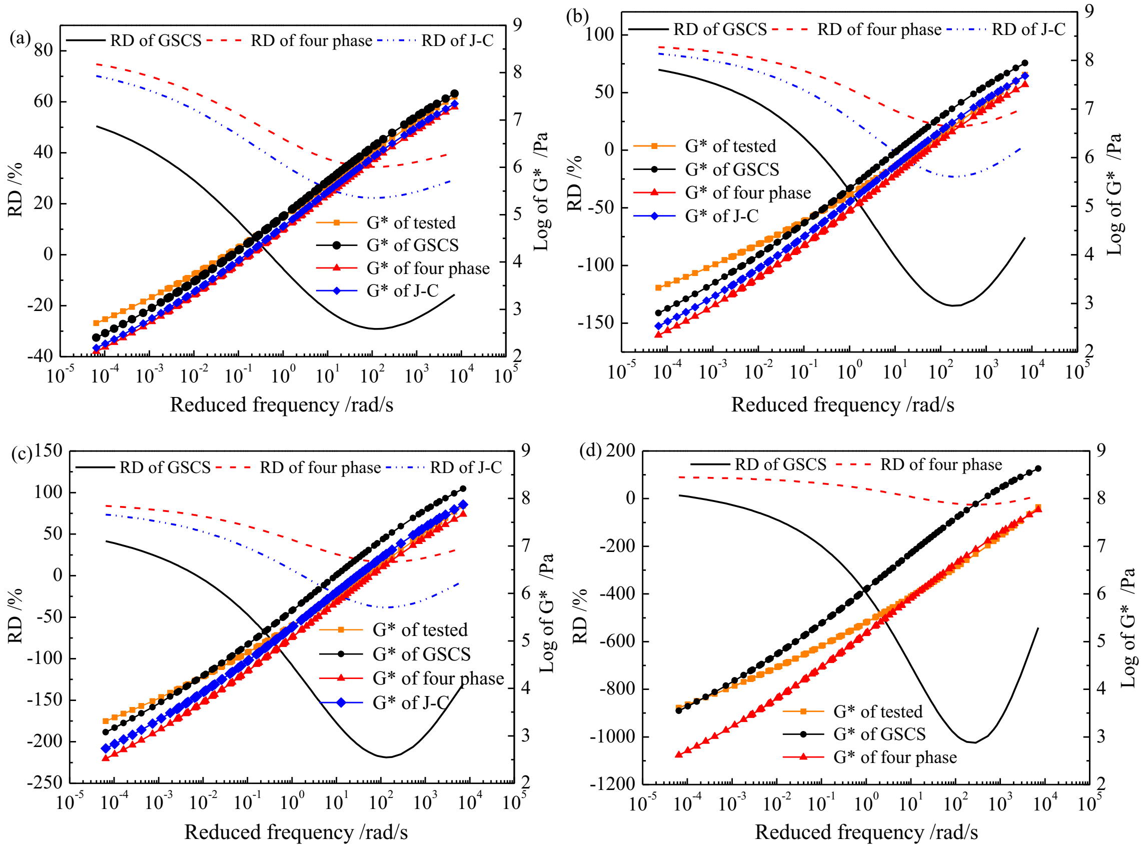

Fig. 10. Comparison of complex modulus master curves and relative difference of the tested and predicted results of SBS modified asphalt mastics with filler volume fraction of (a) 0.23; (b) 0.38; (c) 0.53; (d) 0.68.

(3) When the filler volume fraction was greater than 0.53, the deviations increased severely for the GSCS and four phase model. What is more, the predicted complex modulus value of the J-C model was negative. It means that the complex shear modulus of mastic with large filler volume fraction could not be predicted J-C model.

4.3. Limitation of the three models

For the GSCS model, the application of the calibrated effect filler volume fraction that took the adsorbed rigid layer of asphalt on a filler into account significantly improved the prediction accuracy [7]. However, in this model, the apparent rigid layer thickness was determined according solely to the properties of the mineral filler, without considering the effects of the filler volume fraction on the thickness of the rigid layer. This disadvantage caused the deterioration of prediction with the increasing of the filler volume fraction. Analysis of the predicted master curve also showed that the GSCS calculation accuracy was most significantly affected by the frequency in the comparative results of the three models. In addition to the above shortcomings, there is another obvious limitation of the GSCS model. According to GSCS model, the effective stiffness of asphalt mastic was derived from the relation between the loading and the averaged deformation of the solid particles. The calculation is based on the solution for one particle. This makes the GSCS an effective method of modulus prediction for asphalt mastic with a small filler volume fraction, yet with the increasing of filler volume fraction, the interaction between fillers gradually become stranger and stranger, which makes it impossible to calculate the effective modulus from the solution for one particle.

According to Pei's study on the prediction precision of the J-C model, he found that Young's modulus coefficient ζ which is related to the overall interaction of particles, was decided by the filler volume fraction and the shape of particles. Using a radial distribution function, the value of Young's modulus can be obtained by an integral equation. The radial distribution function is related to particle number densities, particle radius and the distances between particles. Therefore, for asphalt mastic, the calculation of Young' modulus is time-consuming and complicated even if the shape of mineral filler is assumed to be spherical. For this reason, a roughly estimated value, ζ, is used as the parameter to represent the particle interaction, which eventually lead to the increases of the uncertainty of the prediction of J-C model. This effect of ζvalue on the predicted modulus is not significant for mastic with small filler volume fraction, however, with the increasing of filler volume fraction, the effect of ζon the result of modulus prediction are more and more obvious. Still, there is no quantitative relationship between the ζ value and filler volume fraction. What is more, it should be noted that for mastics with a filler volume fraction of 0.68, the J-C predictions are lacking as the predicted modulus appears negative, and even Young's modulus coefficient was assigned an infimum value of 1/24 based on J.W. Ju's research on micromechanics of particle-reinforced composites [17]. This indicates that the J-C model can only predict mastic modulus within a limited range (low and moderate) of filler volume fraction.

Compared with the GSCG and J-C model, the four-phase model generally shows a more precise forecast of mastic complex modulus. However, this model has some defects that cannot be ignored. First, this model employed so many parameters, the validation of which is still open, and the introduction of those parameters give raise to the uncertainty and complexity of the model. Secondly,

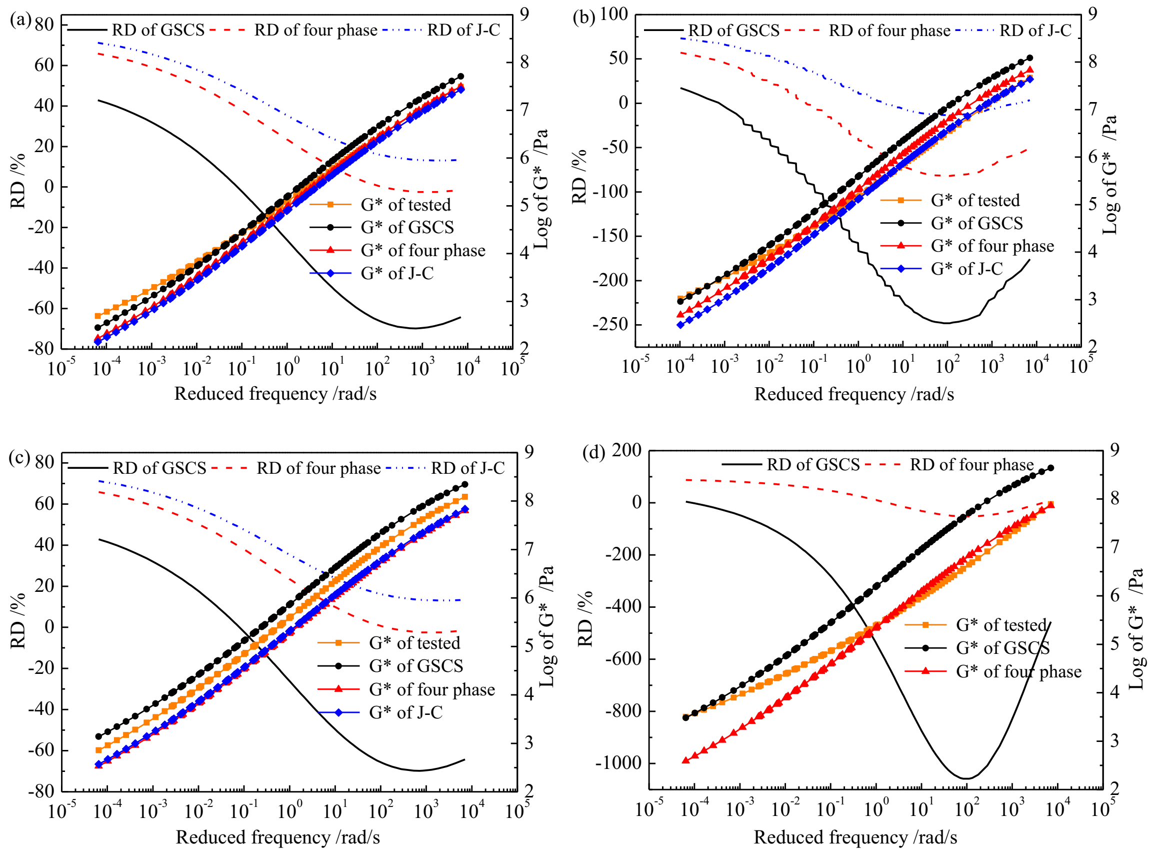

Fig. 11. Comparison of complex modulus master curves and relative difference of the tested and predicted results of HV asphalt mastics with filler volume fraction of (a) 0.23; (b) 0.38; (c) 0.53; (d) 0.68.

prediction of the four-phase model could only be obtained with the help of a specific software program, and even so, that is a time-consuming process. So it is not very convenient to use in practice. Also, just as the GSCS model, the modulus prediction of four-phase model is also based on the assumption that the fillers as well as the rigid layers of asphalt on the surface are isolated as an infinitesimal volume element and the rest of the material is homogenized as a uniform material. The averaged strain of mineral fillers is derived from the solution for one particle embedded in the infinite domain. This makes the deviations increase severely as the filler volume fraction grows up to 0.53, at which the inter-particle interaction in mastic aggravated and the modulus cannot be appropriately predicted by the four phase model.

5. Conclusion

Three GSCS, four-phase and J-C models are presented for the prediction of the complex modulus of mastics fabricated by four different asphalt binders and mineral fillers of four different volume fractions. The complex modulus and phase angle of asphalt binders are obtained by experimental tests and their Poisson ratio is defined as 0.45. The modulus of mineral filler and its Poisson ratio are defined as 1.9×10^{10}Pa and 0.35, respectively. Given these properties of the constituent materials and filler volume fractions, the complex shear modulus of mastic is calculated. By analyzing and comparing the relative differences between the results obtained from experimental tests and prediction models, the following conclusions are reached.

Predicted results of the three models agreed well with the experimental results of mastics with low and moderate filler volume fractions, but the prediction accuracy deteriorated as the filler volume fraction increased.

These three models underestimated the complex modulus of polymer modified asphalt mastic at a frequency less than 1 rad/s and had lower prediction accuracy for modified asphalt mastics than virgin asphalt mastics with the same filler volume fraction.

The GSCS model has a satisfactory prediction at a low filler volume fraction compared with the other two models but its calculation accuracy is most significantly affected by frequency. The J-C model could also predict the effective properties of mastics with a low filler volume fraction, but it could not calculate the complex modulus of mastic with a filler volume fraction of more than 0.53. In the J-C model, Young's modulus coefficient was the main factor that affected the prediction; however, the determination of this coefficient was uncertain, which resulted in uncertainty in the predictions.

Compared with the GSCS and J-C models, the four-phase model was less affected by frequencies or filler volume fractions and showed a more precise forecast of the complex shear modulus of mastics with moderate and high filler volume fractions. However, the calculation process is complicated and time-consuming. The parameters of the model can only be obtained with the help of specific software program, which makes it inconvenient to use in practice.

Therefore, further research should be conducted to simplify these models, improve their accuracy, or put forward new models to better predict the effective properties of asphalt mastic.

Acknowledgements

This project was supported by Natural Science Found Committee (NSFC) of China, China (No. 51608045), Outstanding Youth Fund, Changàn University, China (No. 310831163501), China Postdoctoral Science Foundation, China (Grant No. 2017M613035), the

Science and Technology Plan Projects in Guangxi Province, China (No. AC16380112), the Basic Research Project in Qinghai Province, China (No. 2017-ZJ-715), Key Research and Development Program of Shanxi Province, China (No. 2018SF-403) and the Fundamental Research Funds for the Central Universities of China, China (No. 300102318401). The authors gratefully acknowledge support from Changàn University and Natural Science Found Committee.

References

[1] B.S. Underwood, Y.R. Kim, Microstructural investigation of asphalt concrete for performing multiscale experimental studies, Int. J. Pavement Eng. 14 (2013) 498–516.
[2] B.S. Underwood, Y.R. Kim, Experimental investigation into the multiscale behaviour of asphalt concrete, Int. J. Pavement Eng. 12 (2011) 357–370.
[3] B.S. Underwood, Y.R. Kim, Microstructural association model for upscaling prediction of asphalt concrete dynamic modulus, J. Mater. Civ. Eng. 25 (2013) 1153–1161.
[4] J. Li, F. Ni, Q. Lu, Experimental investigation into the multiscale performance of asphalt mixtures with high contents of reclaimed asphalt pavement, J. Mater. Civ. Eng. 30 (2018).
[5] C. Pichler, R. Lackner, E. Aigner, Generalized self-consistent scheme for upscaling of viscoelastic properties of highly-filled matrix-inclusion composites – application in the context of multiscale modeling of bituminous mixtures, Compos. Part B 43 (2012) 457–464.
[6] W.G. Buttlar, R. Roque, Evaluation of empirical and theoretical models to determine asphalt mixture stiffnesses at low temperatures, in: Proceedings of the 1996 Conference of the Association of Asphalt Paving Technologies: Asphalt Paving Technology, March 18, 1996–March 20, 1996, Assoc of Asphalt Paving Technologists, Baltimore, MD, USA, 1996, pp. 99–141.
[7] W.G. Buttlar, D. Bozkurt, G.G. Al-Khateeb, A.S. Waldhoff, Understanding asphalt mastic behavior through micromechanics, Transp. Res. Rec. (1999) 157–169.
[8] G.G. Ai-Khateeb, M.F. Irfaeya, T.S. Khedaywi, A new simplified micromechanical model for asphalt mastic behavior, Constr. Build. Mater. 149 (2017) 587–598.
[9] E. Hesami, B. Birgisson, N. Kringos, Numerical and experimental evaluation of the influence of the filler-bitumen interface in mastics, Mater. Struct. 47 (2014) 1325–1337.
[10] M. Guo, Y.Q. Tan, Y. Hou, L.B. Wang, Y.Q. Wang, Improvement of evaluation indicator of interfacial interaction between asphalt binder and mineral fillers, Constr. Build. Mater. 151 (2017) 236–245.
[11] M. Guo, A. Motamed, Y. Tan, A. Bhasin, Investigating the interaction between asphalt binder and fresh and simulated RAP aggregate, Mater. Des. 105 (2016) 25–33.
[12] M. Guo, Y. Tan, J. Yu, Y. Hou, L. Wang, A direct characterization of interfacial interaction between asphalt binder and mineral fillers by atomic force microscopy, Mater. Struct. 50 (2017).
[13] M. Guo, A. Bhasin, Y. Tan, Effect of mineral fillers adsorption on rheological and chemical properties of asphalt binder, Constr. Build. Mater. 141 (2017) 152–159.
[14] M. Guo, Y. Tan, Interaction between asphalt and mineral fillers and its correlation to mastics viscoelasticity, 2019.
[15] J. Zhang, X. Li, G. Liu, J. Pei, Effects of material characteristics on asphalt and filler interaction ability, Int. J. Pavement Eng. 20 (2017) 928–937.
[16] B.S. Underwood, Y.R. Kim, A four phase micro-mechanical model for asphalt mastic modulus, Mech. Mater. 75 (2014) 13–33.
[17] J.W. Ju, T.M. Chen, Effective elastic moduli of two-phase composites containing randomly dispersed spherical inhomogeneities, Acta Mech. 103 (1994) 123–144.
[18] J.W. Ju, T.M. Chen, Micromechanics and effective moduli of elastic composites containing randomly dispersed ellipsoidal inhomogeneities, Acta Mech. 103 (1994) 103–121.
[19] J. Pei, Z. Fan, P. Wang, J. Zhang, B. Xue, R. Li, Micromechanics prediction of effective modulus for asphalt mastic considering inter-particle interaction, Constr. Build. Mater. 101 (2015) 209–216.
[20] J. Zhang, Z. Fan, J. Pei, R. Li, M. Chang, Multiscale validation of the applicability of micromechanical models for asphalt mixture, Adv. Mater. Sci. Eng. (2015).
[21] J. Zhang, X. Li, W. Ma, J. Pei, Characterizing heterogeneity of asphalt mixture based on aggregate particles movements, Iran. J. Sci. Technol. Trans. Civ. Eng. 43 (2018) 81–91.
[22] J. Zhang, Z. Fan, H. Wang, W. Sun, J. Pei, D. Wang, Prediction of dynamic modulus of asphalt mixture using micromechanical method with radial distribution functions, Mater. Struct. 52 (2019).
[23] T. Mori, K. Tanaka, Average stress in matrix and average elastic energy of materials with misfitting inclusions, Acta Metall. 21 (1973) 571–573.
[24] M. Kim, W.G. Buttlar, Differential scheme effective medium theory for hot-mix asphalt |E*| prediction, J. Mater. Civ. Eng. 23 (2011) 69–78.
[25] F. Fakhari Tehrani, J. Quignon, F. Allou, J. Absi, C. Petit, Two-dimensional/three-dimensional biphasic modelling of the dynamic modulus of bituminous materials, Eur. J. Environ. Civ. Eng. 17 (2013) 430–443.
[26] F.F. Tehrani, J. Absi, F. Allou, C. Petit, Investigation into the impact of the use of 2D/3D digital models on the numerical calculation of the bituminous composites' complex modulus, Comput. Mater. Sci. 79 (2013) 377–389.
[27] F.F. Tehrani, J. Absi, F. Allou, C. Petit, Micromechanical modelling of bituminous materials' complex modulus at different length scales, Int. J. Pavement Eng. 19 (2018) 685–696.
[28] P. Hajikarimi, F.F. Tehrani, F.M. Nejad, J. Absi, A. Khodaii, M. Rahi, C. Petit, Mechanical behavior of polymer-modified bituminous mastics. II: numerical approach, J. Mater. Civ. Eng. 31 (2019).
[29] K. Yan, H. Xu, H. Zhang, Effect of mineral filler on properties of warm asphalt mastic containing Sasobit, Constr. Build. Mater. 48 (2013) 622–627.
[30] Y.R. Kim, D.N. Little, Linear viscoelastic analysis of asphalt mastics, J. Mater. Civ. Eng. 16 (2004) 122–132.
[31] H.M. Yin, W.G. Buttlar, G.H. Paulino, H. Di Benedetto, Assessment of existing micro-mechanical models for asphalt mastics considering viscoelastic effects, Road Mater. Pavement Des. 9 (2008) 31–57.
[32] L.C. Brinson, W.S. Lin, Comparison of micromechanics methods for effective properties of multiphase viscoelastic composites, Compos. Struct. 41 (1998) 353–367.
[33] R.M. Christensen, K.H. Lo, Solutions for effective shear properties in three phase sphere and cylinder models, J. Mech. Phys. Solids 27 (1979) 315–330.
[34] Y. Cheng, J. Tao, Y. Jiao, G. Tan, Q. Guo, S. Wang, P. Ni, Influence of the properties of filler on high and medium temperature performances of asphalt mastic, Constr. Build. Mater. 118 (2016) 268–275.
[35] X. Zhu, Z. Yang, X. Guo, W. Chen, Modulus prediction of asphalt concrete with imperfect bonding between aggregate-asphalt mastic, Compos. Part B 42 (2011) 1404–1411.
[36] N.I.M. Yusoff, F.M. Jakarni, V.H. Nguyen, M.R. Hainin, G.D. Airey, Modelling the rheological properties of bituminous binders using mathematical equations, Constr. Build. Mater. 40 (2013) 174–188.
[37] M. Cholewinska, M. Iwanski, G. Mazurek, The impact of aging on the bitumen stiffness modulus using the CAM model, Baltic J. Road Bridge Eng. 13 (2018) 34–39.